https://doi.org/10.1016/j.apacoust.2016.08.020 This is the Pre-Published Version.

Technical Note

An extended neck versus a spiral neck of the Helmholtz resonator

Chenzhi Cai, Cheuk-Ming Mak* and Xiaofeng Shi

Department of Building Services Engineering, The Hong Kong Polytechnic University, Hung Hom, Kowloon, Hong Kong

chenzhi.cai@connect.polyu.hk, cheuk-ming.mak@polyu.edu.hk

*Corresponding author.
E-mail Address: cheuk-ming.mak@polyu.edu.hk (C.M.Mak).
Telephone: +852 2766 5856
Fax: +852 2765 7198

Abstract

This paper focuses on improving the noise attenuation performance of the Helmholtz resonator (HR) at low frequencies with a limited space. An extended neck or a spiral neck takes the place of the traditional straight neck of the HR. The acoustic performance of the HR with these two types of necks is analyzed theoretically and numerically. The length correction factor is introduced through a modified one-dimensional approach to account for the non-planar effects that result from the neck being extended into the cavity. The spiral neck is transformed to an equivalent straight neck, and the acoustic performance is then derived by a one-dimensional approach. The theoretical prediction results fit well with the Finite Element Method (FEM) simulation results. Without changing the cavity volume of the HR, the resonance frequency shows a significant drop when the extended neck length or the spiral neck length is increased. The acoustic characteristics of HRs with these two different neck types have a potential application in noise control, especially at low frequencies within a constrained space.

Keywords: Helmholtz resonator, extended neck, spiral neck, noise control

1. Introduction

A ventilation ductwork system is an essential system in buildings that provides conditioned or fresh air to indoor environments so as to ensure good indoor air quality. However, it is common to encounter a duct-borne noise problem in these ventilation systems [1,2]. The unpleasant noise in the ventilation ductwork system can be a disturbance to human activities. It is therefore important to reduce duct-borne noise, especially the low-frequency and broadband noise in the ventilation ductwork system [3]. A dissipative silencer is usually adopted to control noise at mid to high frequencies. However, it is not effective for low-frequency noise control [4]. In recent years, active noise control has become a rapidly developing area of duct-borne noise control. An active noise control system can provide environmental-adaptive noise attenuation, especially at low frequencies. Nevertheless, there are still some problems related to its reliability and high cost [5,6]. For these reasons, the Helmholtz resonator (hereafter, HR) is still widely used as an effective silencer for low-frequency duct-borne noise control due to its characteristics of being tunable, durable, and affordable [7,8]. Therefore, a good design for a Helmholtz resonator is important for noise attenuation in ventilation ductwork systems.

Many researchers and engineers around the world have devoted their attention to improving the attenuation performance of the HR. A lot of achievements have been made and are documented in numerous pieces of literature. Chanaud [9] examined the effects of different orifice shapes and cavity geometries on the resonance frequency of the HR. Tang and Sirignano [10] investigated various neck lengths of the HR, and their results showed that the resonance frequency of the HR was reduced by increasing its neck length.

To improve the sound absorption capacity of the HR in a limited space, Selamet and Lee [11] proposed a HR with an extended neck and examined the effects of length, shape, and perforation of neck extension on acoustic performance. Selamet et al. [12] then presented another approach by lining the HR with fibrous material to improve attenuation performance without changing the geometries of the HR. Pillai and Ezhilarasi [13] investigated the acoustic performance of HRs with tapered necks both experimentally and theoretically. Shi and Mak [14] proposed a HR with a spiral neck to improve attenuation performance by using a curvature effect on the spiral neck.

While the HR is known to be an effective silencer at low frequencies, sometimes its application may be limited by space. It is important to shift the resonance frequency when there is a space constraint. This paper focuses on improving the noise attenuation performance of the HR at low frequencies when there is limited space. A spiral neck or an extended neck may by a feasible way to shift the resonance frequency in such situations. The extended neck will lower the resonance frequency without an extra cavity volume requirement, and the spiral neck can make the neck as long as possible under a space constraint to reduce the resonance frequency. The acoustic performance of HRs with these two types of necks is analyzed both theoretically and numerically. A modified one-dimensional (1D) analytical approach with a length correction factor is used in this paper to accurately predict the acoustic performance of an HR with an extended neck. The length correction factor is introduced due to the apparent multidimensional sound field inside the cavity of an HR with an extended neck [15]. The length correction factor is obtained using a two-dimensional (2D) analytical approach. The wave propagation of an HR with a spiral neck is also analyzed. The curvature of the spiral neck changes the

impedance, and the spiral neck can then be considered equivalent to a straight neck with a corrected neck length and cross-section area. The spiral neck is then translated to a traditional straight neck, and the acoustic performance is predicted using a 1D analytical approach.

2. Analytical approach of the HR with an extended neck

The sound fields inside an HR with an extended neck are clearly multidimensional. A modified 1D analytical model, which includes a length correction to account for the non-planar effects at the neck-cavity interface, is proposed here to improve the accuracy of the acoustic performance prediction. The length correction is derived using a 2D analytical approach.

A 2D analytical approach is introduced to determine the length correction length. Fig. 1 shows the geometries of the circular concentric HR with an extended neck. The 2D sound wave propagations in both the extended neck and the cavity are governed by the Helmholtz equation in cylindrical coordinates as:

$$\nabla^2 P(r,x) + k^2 P(r,x) = 0 \tag{1}$$

where p is the sound pressure and k is the wave number. The sound pressure and particle velocity can be solved by Eq. (1) as [16]:

$$P_i(r,x_i) = \sum_{n=0}^{+\infty} (A_{i,n} e^{-jk_{i,n}x_i} + B_{i,n} e^{jk_{i,n}x_i}) \psi_{i,n}(r) \tag{2}$$

$$V_i(r,x_i) = \frac{1}{\rho_0 \omega} \sum_{n=0}^{+\infty} k_{i,n} (A_{i,n} e^{-jk_{i,n}x_i} - B_{i,n} e^{jk_{i,n}x_i}) \psi_{i,n}(r) \tag{3}$$

$$k_{i,n} = \begin{cases} \sqrt{k_0{}^2 - (\alpha_{1,n}/a_i)^2}, k_0 > \alpha_{1,n}/a_i \\ -\sqrt{k_0{}^2 - (\alpha_{1,n}/a_i)^2}, k_0 < \alpha_{1,n}/a_i \end{cases} \tag{4}$$

where $i = 1, 2, 3$ represents different coordinate axis x domains, $A_{i,n}$ and $B_{i,n}$ represent the modal amplitudes corresponding to components traveling in positive and negative directions in different domains, respectively, ρ_0 represents the air density, $k_{i,n}$ represents the wave number, k_0 represents the wave number of the zero mode, and $\psi_{i,n}(r)$ represents the eigenfunction. The eigenfunction $\psi_{i,n}(r)$ is given as:

$$\psi_{i,n}(r) = \begin{cases} J_0(\alpha_{i,n}\frac{r}{a_i}), & i = 1,3 \\ J_0(\alpha_{2,n}\frac{r}{a_2}) - \frac{J_1(\alpha_{2,n})}{Y_1(\alpha_{2,n})} Y_0(\alpha_{2,n}\frac{r}{a_2}), & i = 2 \end{cases} \tag{5}$$

where J_m is the Bessel function of the first kind and order m, Y_m is the Bessel function of the second kind and order m, and $\alpha_{i,n}$ is the root matching the rigid wall condition of $\psi_{i,n}(r) = 0$.

The walls of the neck and the cavity are set to be rigid. At $x_2 = 0$ or $x_3 = l_r$, the rigid wall condition gives $v_2 = 0, v_3 = 0$. At $x_1 = l_e + l_n$ or $x_3 = 0$, the pressure continuity condition at neck-cavity interface gives $P_1 = P_3$. Similarly, at $x_2 = l_e$ or $x_3 = 0$, it gives $P_2 = P_3$. The volume velocity continuity condition at $x_1 = l_e + l_n$ or $x_3 = 0$ gives $V_1 S_n + V_2(S_c - S_n) = V_3 S_c$. Set the relation of initial oscillation sound pressure P_0 and particle velocity V_p at $x_1 = 0$ as $P_0 = \rho_0 c_0 V_p = 1$. c_0 represents the sound speed. Then all unknown $A_{i,n}$ $B_{i,n}$ can be obtained by combining all the boundary conditions above.

The frequency range considered in this paper is well below the cut-off frequency of the resonator neck and the cavity. This means that the non-planar wave excited at the abrupt cross-section change (the neck-cavity interface) will decay exponentially.

Therefore, it is assumed that only planar waves exist in the HR. The multidimensional effects associated with evanescent high modes at a sudden area change are considered the "length correction factor." As a consequence, Eq. (2) and Eq. (3) can be simplified as:

$$P_i(r, x_i) = A_{i,0} e^{-jk_0 x_i} + B_{i,0} e^{jk_0 x_i} \tag{6}$$

$$V_i(r, x_i) = \frac{1}{\rho_0 c_0} (A_{i,0} e^{-jk_0 x_i} + B_{i,0} e^{jk_0 x_i}) \tag{7}$$

Then, at the neck-cavity interface ($x_1 = l_e + l_n$ or $x_3 = 0$), the discontinuity effects will be equivalent to the equation [17]:

$$P_1 = P_3 + \delta Z S_n V_1 \tag{8}$$

where S_n is neck area, Z is the characteristic impedance of the plane mode given as $Z = j\rho_0 c_0 / S_n$, and δ represents the length correction factor. Combining Eq. (6) and Eq. (7) with Eq. (8) gives:

$$\delta = \left| \frac{P_1 - P_3}{j\rho_0 c_0 V_1} \right| = \left| \frac{(A_{1,0} + B_{1,0}) - (A_{3,0} + B_{3,0})}{jk(A_{1,0} - B_{1,0})} \right| \tag{9}$$

Based on the 2D analytical results, an approximate formula for the length correction factor could be given as:

$$\delta = 0.6165 r_n - 0.7046 r_n^{\,2} / r_c + 0.2051 e^{-1.7226 l_e / r_c} r_n - 0.3749 e^{-1.3012 l_e / r_c} r_n^{\,2} / r_c \tag{10}$$

The approximate δ formula agrees well with the simulation and experimental results for $r_n / r_v < 0.5$ [11,18]. Combining only 1D propagation in the axial x direction in the neck and cavity with regard to the effects of the non-planar wave as length correction factor δ, the transmission loss of a side branch HR with an extended neck can be expressed as:

$$TL = 10\log_{10}\left[1+\left(\frac{S_n}{2S_d}\frac{\tan k(l_n+l_e+\delta)+\left(S_c/S_n\right)\tan k(l_c-\delta)}{1-\left(S_c/S_n\right)\tan k(l_c-\delta)\tan k(l_n+l_e+\delta)}\right)^2\right] \tag{11}$$

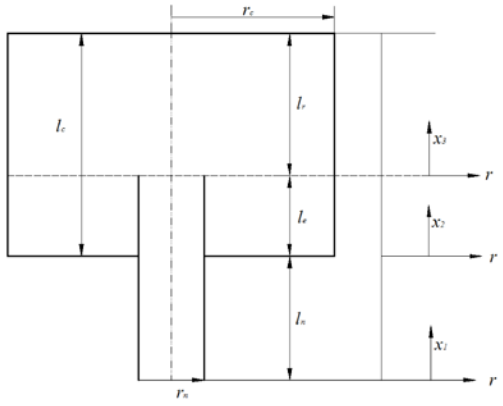

Fig. 1 Helmholtz resonator with extended neck.

3. Analytical approach of HR with a spiral neck

The traditional short neck is replaced by a spiral neck to make the neck as long as possible when there is a space constraint. Meanwhile, the curvature of the spiral neck changes the impedance, and it can then be considered equivalent to the traditional straight neck. For these reasons, this kind of HR can improve noise reduction performance at low frequencies within a limit space.

Fig. 2 (a) illustrates a HR with a spiral neck. The spiral neck can be divided into three parts: two straight tubes of lengths L_I and L_{II} respectively, and the spiral tube, which takes N turns of total length $L_{III} = N*2\pi*R_0$, as shown in Fig. 2 (b). The cross-section area of these three parts is the constant S_n. The particle velocity along the toroidal axis in the spiral tube is determined by the radial dependence of the sound pressure and the curvature dependence of the sound pressure. However, the radial dependence of the sound pressure is quite small due to the low frequency range considered in this paper.

This means that the sound pressure remains the same over the cross-section area [19]. Therefore, the particle velocity is simplified as:

$$v(R_0,\phi)=\frac{-1}{j\omega\rho_0}\frac{1}{R_0}\frac{\partial p}{\partial\phi} \tag{12}$$

where p is the sound pressure, ω is the angular frequency, ρ_0 is the air density, ϕ is the curvature angle, and R_0 is the distance from the point of the curvature center.

The curvature changes the impedance of the spiral tube, and it can then be considered equivalent to a straight tube. For the spiral tube with cross-section area S_n and length L_{III} shown in Fig. 2 (b), the equivalent straight tube with cross-section area S_n' and L_{III}' is expressed as:

$$S_n' = S_n/\sqrt{F}\ ,\ L_{III}' = L_{III}\sqrt{F} \tag{13}$$

where $F=0.5(r_0/R_0)^2\Big/(1-\sqrt{1-(r_0/R_0)^2})$ is the equivalent coefficient as a result of the curvature in the tube and r_0/R_0 indicates the abruptness of the bend and its effects on the equivalent coefficient.

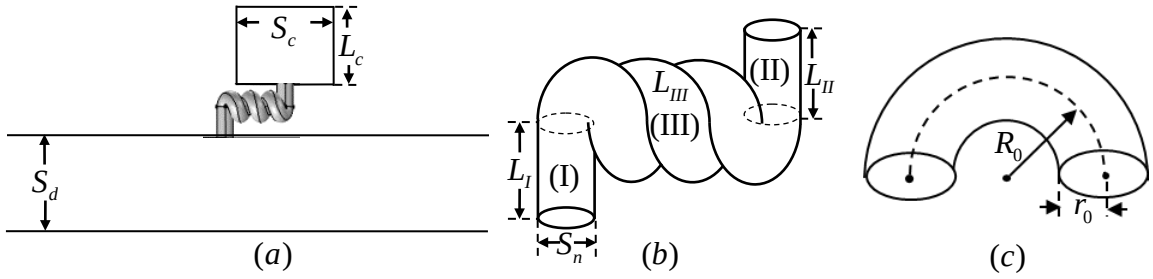

Fig. 2 (*a*) A Helmholtz resonator with a spiral neck. (b) The spiral neck with three turns. (c) A section of the curved tube.

The equivalent coefficient F is practically less than unity, which means that the equivalent straight tube has a larger area ($S_n' > S_n$) and a shorter length ($L_{III}' < L_{III}$). The spiral neck could therefore be considered a combination of three connected straight tubes in a theoretical analysis. The equivalent theoretical model of a HR with a spiral neck is shown in Fig. 3.

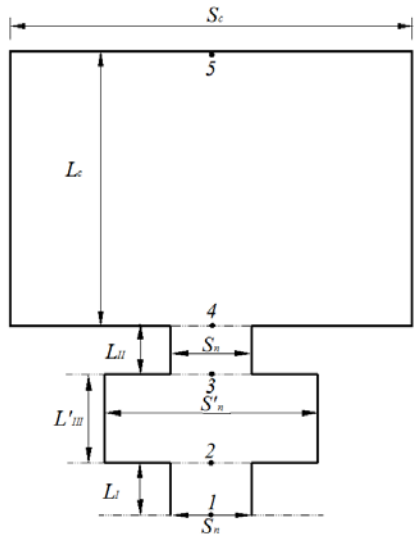

Fig. 3 The equivalent Helmholtz resonator.

The frequency range considered here is well below the cut-off frequency, so only planar waves propagate in the neck and cavity. The relation of point 1 to point 5 could be obtained through the transfer matrix method [20] as:

$$\begin{bmatrix} P_1 \\ \rho_0 S_n V_1 \end{bmatrix} = \begin{pmatrix} \cos(k_0 L_I) & j(\frac{c_0}{S_n})\sin(k_0 L_I) \\ j(\frac{S_n}{c_0})\sin(k_0 L_I) & \cos(k_0 L_I) \end{pmatrix} \begin{pmatrix} \cos(k_0 L_{III}') & j(\frac{c_0}{S_n'})\sin(k_0 L_{III}') \\ j(\frac{S_n'}{c_0})\sin(k_0 L_{III}') & \cos(k_0 L_{III}') \end{pmatrix} \begin{pmatrix} \cos(k_0 L_{III}) & j(\frac{c_0}{S_n})\sin(k_0 L_{III}) \\ j(\frac{S_n}{c_0})\sin(k_0 L_{III}) & \cos(k_0 L_{III}) \end{pmatrix} \begin{pmatrix} \cos(k_0 L_c) & j(\frac{c_0}{S_c})\sin(k_0 L_c) \\ j(\frac{S_c}{c_0})\sin(k_0 L_c) & \cos(k_0 L_c) \end{pmatrix} \begin{bmatrix} P_5 \\ \rho_0 S_c V_5 \end{bmatrix} \tag{14}$$

Eq. (14) could be simplified as:

$$\begin{bmatrix} P_1 \\ \rho_0 S_n V_1 \end{bmatrix} = \begin{pmatrix} T_{11} & T_{12} \\ T_{21} & T_{22} \end{pmatrix} \begin{bmatrix} P_5 \\ \rho_0 S_c V_5 \end{bmatrix} \tag{15}$$

where P_1 , V_1 and P_5 , V_5 are the sound pressures and particle velocities at point 1 and point 5, respectively. Assuming the walls of the cavity are rigid, the particle velocity at point 5 equals zero ($V_5 = 0$). The impedance of HR with a spiral neck could be derived from Eq. (15) as:

$$Z_r = \frac{P_1}{V_1 S_n} = \rho_0 \frac{T_{11}}{T_{21}} \tag{16}$$

Once the resonator impedance has been obtained, the transmission of a side-branch HR with a spiral neck can be described as:

$$TL = 20 \log_{10} \left| \frac{Z_r}{\rho_0 c_0 / 2S_d + Z_r} \right| \tag{17}$$

4. Results and discussion

For a HR with fixed cavity volume, the effects of the two neck types on transmission loss are each analyzed. For a side-branch HR with an extended neck, the modified 1D analytical approach is used for an accurate prediction. The theoretical model of HR with a spiral neck is translated to an equivalent HR with a concentrated straight neck. The theoretical predictions are compared to the FEM simulation results.

4.1 Validation of the predicted transmission loss due to the HR with an extended neck

The HR with an extended neck is shown in Fig. 1. The geometries of the HR used in this paper are: cavity length $l_c = 21cm$, cavity radius $r_c = 6.6cm$, neck radius $r_n = 1cm$, and base neck length $l_n = 8cm$. The cross-section area of the main duct is $S_d = 36cm^2$. The effects of extension length l_e on the transmission loss are studied first.

The transmission loss of a HR with different extension lengths that is analyzed by a modified 1D approach is shown in Fig. 4. It can be seen that with the increase in neck extension length, the resonance frequency decreases with a narrower attenuation band. Fig. 5 compares the predicted results to the FEM simulation results. It is shown that the modified 1D analytical approach predictions fit well with the FEM simulation results. Note that a 15.08cm change in extension length results in a 22 Hz shift in the resonance frequency, while the resonance frequency of a HR without an extended neck is only 59Hz, as shown in Fig. 4. The alteration in resonance frequency is apparent and significant at low frequency range. Furthermore, no change in cavity volume is required for the reduction in resonance frequency.

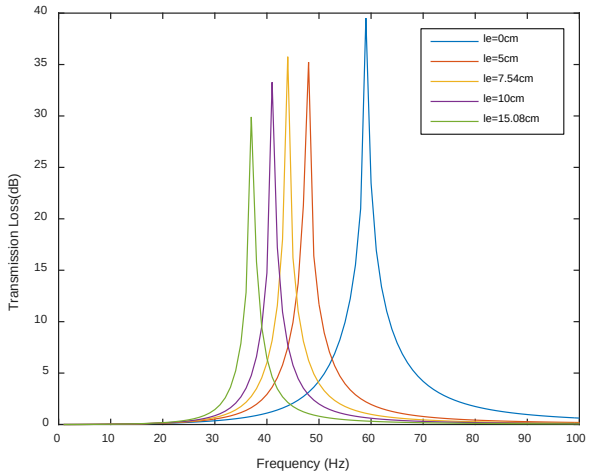

Fig. 4 Transmission loss of the HR with different extension neck lengths.

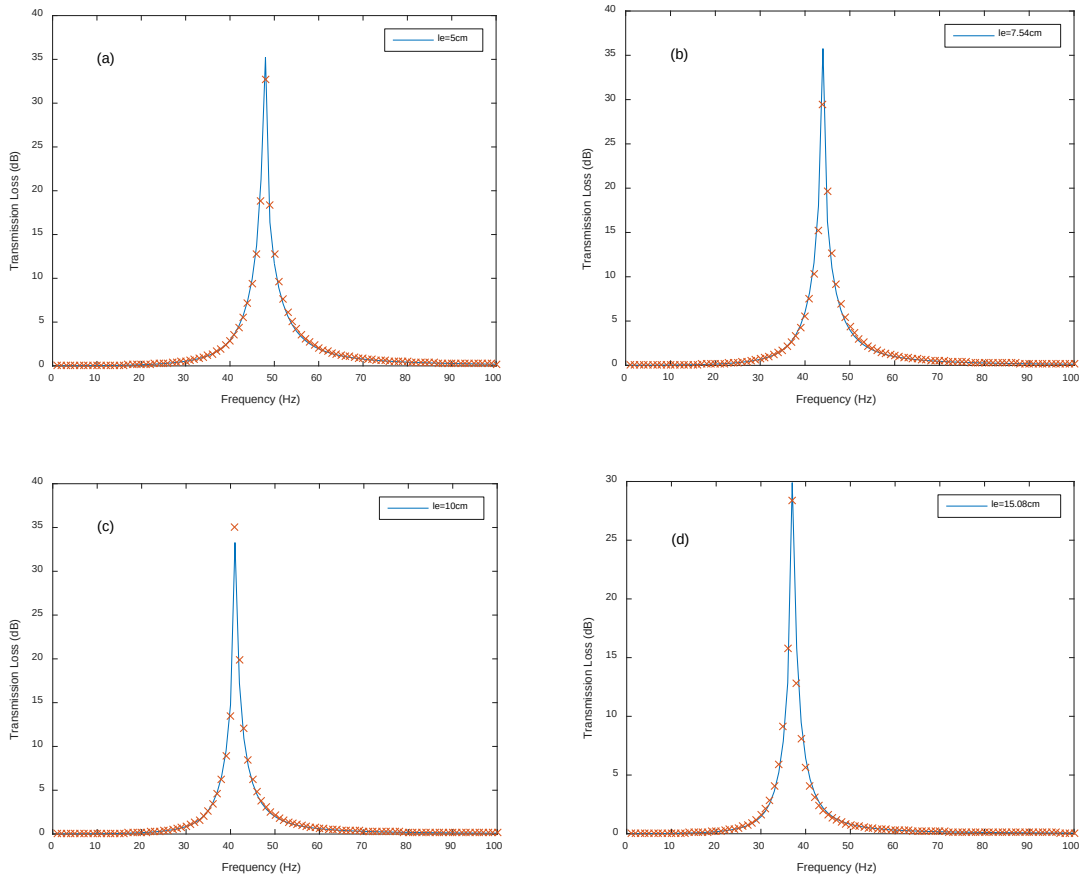

Fig. 5 Comparison of the analytical approach predictions and the FEM simulation for different extension neck lengths (solid lines represent the theoretical prediction, and dotted crosses represent the FEM simulation results).

Selamet and Lee [11] experimented on the Helmholtz resonator with different extension lengths. The geometries of their experimental HR are: $l_v = 20.32cm$, $r_v = 7.62cm$, $r_n = 2cm$, $l_n = 8.5cm$, and $S_d = 18.49cm^2$, which are different from the geometries used in this paper. Fig. 6 illustrates a good agreement between the predictions of the modified 1D analytical approach and the results of Selamet and Lee's experiment. Their experimental results are directly extracted from their publication to verify the accuracy of the modified 1D method. Similarly, a 15cm extension length into the cavity results in a

33 Hz shift in resonance frequency without a change in the cavity volume, which is distinct when compared to the resonance frequency of 98 Hz for a HR without the extended neck.

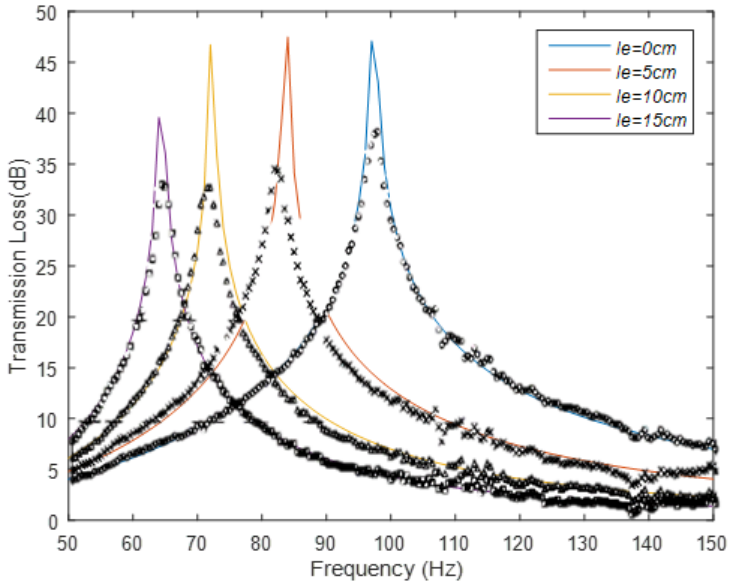

Fig. 6 Comparison of the modified 1D analytical approach predictions and the experiment for a Helmholtz resonator with different extension lengths (the dotted symbols represent the experiment's results).

4.2 Validation of the predicted transmission loss due to the HR having a spiral neck

The HR with a spiral neck is shown in Fig. 2. The geometries of the HR are: cavity length $l_c = 21cm$, cavity radius $r_c = 6.6cm$, fixed neck radius $r_n = 1cm$, straight tube length $L_I = L_{II} = 4cm$, $R_0 = 1.2cm$, and length of spiral tube $L_{III} = N*2\pi R_0 = N*7.54cm$ (length of each turn is $7.54cm$). The cross-section area of the main duct is $S_d = 36cm^2$. The N is an integer here, and it indicates the turns of the spiral tube. When *N* equals zero, this means that the spiral tube is non-existent and the neck only contains two straight tubes, which actually make it a traditional straight neck. Besides, the spiral tube could be

treated as equivalent to a straight tube in a theoretical model, as shown in Fig. 3, when $N \neq 0$.

The predicted transmission loss of a HR with different turn number ($N = 0,1,2,3,4$) is exhibited in Fig. 7. Added spiral turns will decrease the resonance frequency and narrow the attenuation band, as well. Fig. 8 compares the prediction results with the FEM simulation results, and the prediction results are in good agreement with the FEM simulation results. The resonance frequency of the HR without a spiral neck ($N = 0$) is 59Hz. However, the resonance frequency decreases to 45Hz, 38Hz, 34Hz, and 30 Hz for $N = 1,2,3,4$, respectively. This also means that a spiral tube with 30.16cm ($N = 4$) change results in a 29Hz decrease in the resonance frequency without changing the cavity volume. The effects of a spiral tube on the resonance frequency are obvious, especially at a low frequency range. Moreover, more turns will result in a much lower resonance frequency. When the total neck length is comparable to the wavelength of oscillation, for instance $N = 4$ in this paper, the peak amplitude will increase due to the long neck length [10].

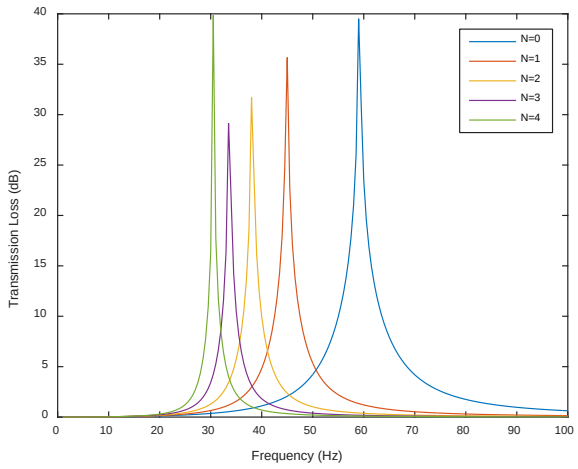

Fig. 7 Transmission loss of a Helmholtz resonator with a spiral neck.

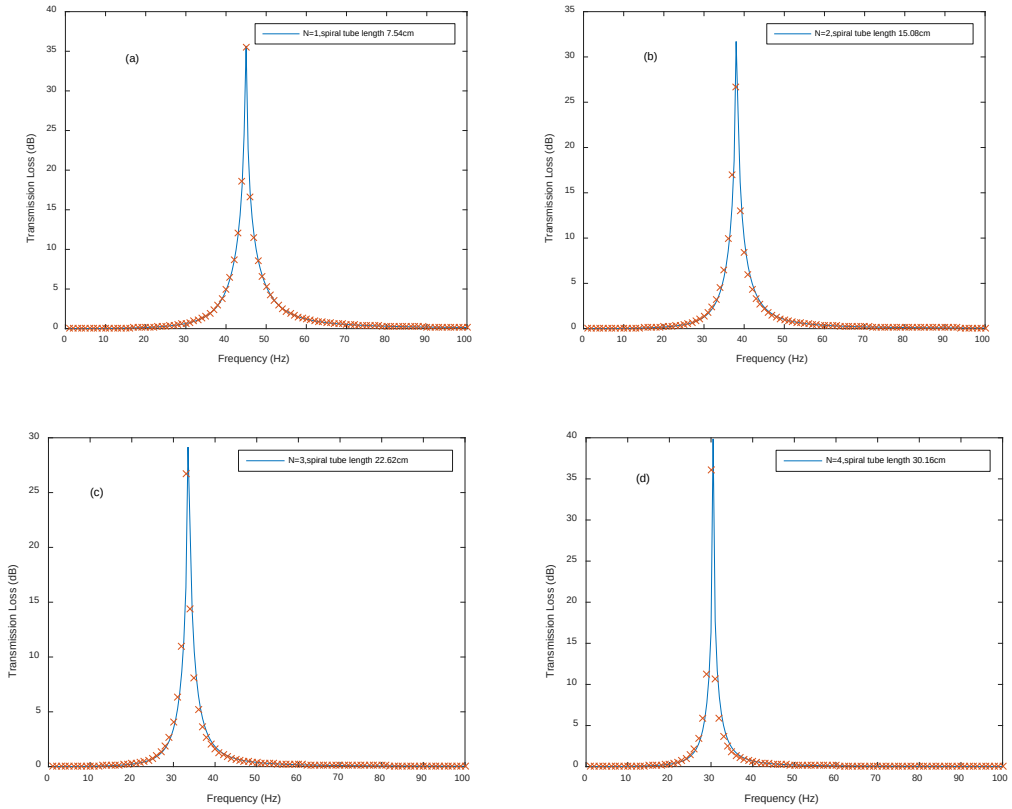

Fig. 8 Comparison of predictions with FEM simulation for different spiral tube lengths (solid lines represent the theoretical prediction, and dotted crosses represent the FEM simulation results).

4.3 Transmission loss comparison of HRs with different neck types

As described above, the cavity geometries of HRs with different neck types are the same, as are as the neck radiuses. The relation of the base neck length in Fig. 1 to the length of the two straight tubes in Fig. 2 can be expressed as: $l_n = L_I + L_{II}$. This means that the resonance frequency of the HR without the extended neck or the spiral neck is 59Hz. Fig. 9 compares the amount of transmission loss between the HRs with different neck types. The results show that a 7.54cm and a 15.08cm extension length change or spiral tube length change result in a 14Hz and a 21Hz decrease in the resonance

frequency, respectively. The effect of the extension neck length on resonance frequency is nearly the same as the effect of the spiral tube length on resonance frequency.

The extension length could be changed flexibly to satisfy the required resonance frequency, but it is limit to the cavity length. For the spiral tube, there is no limit to the number of possible turns. The HR with a spiral neck can shift the resonance frequency to a much lower extent by having more turns added. For instance, the spiral tube with $N = 4$ means that the length of the tube comes to 30.16cm, which is much longer than the extension length limitation. However, the length of each turn is invariable at $2\pi R_0$.

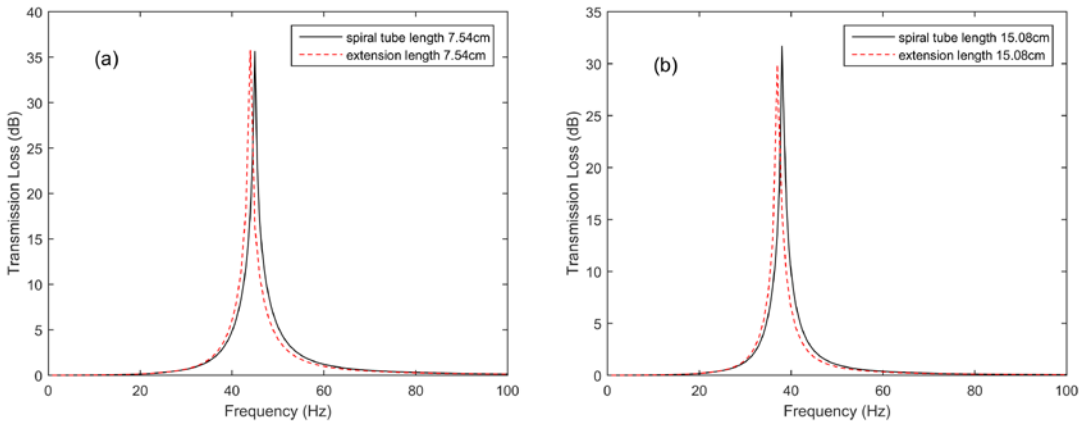

Fig. 9 Comparison of the HR with an extended neck and the HR with a spiral neck (dashed lines represent the HR with an extended neck, and solid lines represent the HR with a spiral neck).

5. Conclusion

This paper focuses on improving the noise attenuation performance of the HR at low frequencies within a constrained space. This paper presents theoretical and numerical studies of a HR with an extended neck and a HR with a spiral neck. The modified 1D analytical approach with length correction factor is used in this paper to make an accurate

acoustic performance prediction of a HR with an extended neck. The length correction factor is introduced to account for the non-planar wave effects. For the HR with a spiral neck, the curvature of the spiral neck changes the impedance, and the spiral neck can then be considered equivalent to a straight neck with a corrected neck length and cross-section area. The spiral neck is then translated to a traditional straight neck, and the acoustic performance prediction is derived using a 1D analytical approach.

The predicted theoretical results fit well with the FEM simulation results. Additionally, the prediction results for the HR with an extended neck also agree nicely with the existing experimental results documented in the literature. With the increasing of the extension length or the spiral neck length, resonance frequency decreases significantly. An identical change in the extension neck length or the spiral neck length will produce the same decrease in resonance frequency. It is clear that a 22Hz decrease in resonance frequency is obtained without changing the cavity volume, a significant difference from the resonance frequency of 59Hz that exists for HRs without these two types of necks. The extension neck length is flexible but limited to the cavity length. Although there is no limit to the spiral neck length, more spiral turns could be added to lengthen the neck. However, the spiral tube length of each turn is fixed. For a certain designed resonance frequency of HR, the utilization of the extended neck or the spiral neck can reduce the cavity volume. The acoustic characteristics of HRs with these two different neck types have a potential application in noise control at low frequencies within a constrained space.

Acknowledgements

The work described in this paper was fully supported by a grant from the Research Grants Council of the Hong Kong Special Administrative Region, China (Project No. PolyU 152116/14E).

References

[1] Mak CM, Wu J, Ye C, Yang J. Flow noise from spoilers in ducts. J Acoust Soc Am 2009;125(6):3756-3765.

[2] Mak CM. A prediction method for aerodynamic sound produced by multiple elements in air duct. J Sound Vib 2005;287(1-2):395-403.

[3] Fry A. Noise Control in Building Services. Oxford: Pergamon; 1987.

[4] Peat KS, Rathi KL. A finite element analysis of the convected acoustic wave motion in dissipative silencers. J Sound Vib 1995;184(3):529-545.

[5] Kuo SM, Morgan DR. Active Noise Control System Algorithms and DSP Implementation. New York: Wiley; 1996.

[6] Hansen CH, Snyder SD. Active Control of Noise and Vibration. London: E&FN Spon; 1997.

[7] Ingard U. On the theory and design of acoustic resonators. J Acoust Sco Am 1953;25: 1037-1061.

[8] Du L, Aborm M, Karlsson M, Knutsson M. Modelling of acoustic resonators using the linearized Navier Stokes equation. SAE Techical Paper 2016;2016-01-1821.

[9] Chanaud RC. Effects of geometry on the resonance frequrncy of Helmholtz resonator. J Sound Vib 1994;178(3):337-348.

[10] Tang PK, Sirignano WA. Theory of a generalized Helmholtz resonator. J Sound Vib 1973;26(2):247-262.

[11] Selamet A, Lee IJ. Helmholtz resonator with extended neck. J Acoust Soc Am 2003;113(4):1975-1985.

[12] Selamet A, Xu MB, Lee IJ, Huff NT. Helmholtz resonator lined with absorbing material. J Acoust Soc Am 2005;117(2):725-733.

[13] Pillai MA, Ezhilarasi D. Improved acoustic energy harvester using tapered neck Helmholtz resonator and piezoelectric cantilever undergoing concurrent bending and twisting. Procedia Eng 2016;144:674-681.

[14] Shi XF, Mak CM. Helmholtz resonator with a spiral neck. Appl Acoust 2015;99:68-71.

[15] Bies DA, Hansen CH. Engineering Noise Control: Theory and Practice. 4th ed. London: Spon Press; 2009.

[16] Munjal ML. Acoustic of Ducts and Mufflers. New York: Wiley; 1987.

[17] Kergomard J. Simple discontinuty in acoustic waveguides at low frequency: cirtical analysis and formula. J Sound Vib 1987;114(3):465-479.

[18] Kang ZX, Ji ZL. Acoustic length correction of duct extension into a cylindrical chamber. J Sound Vib 2008;310(4-5):782-791.

[19] Nederveen CJ. Influence of a toroidal bend on the wind structure tuning. J Acoust Soc Am 1998;104;1616-26

[20] ZL Ji, JZ Sha. Four-pole parameters of a duct with Low Mach number flow. J Acoust Soc Am 1995;98(5):2848-2850.

Figure captions

Fig. 1 Helmholtz resonator with extended neck.

Fig. 2 (*a*) A Helmholtz resonator with a spiral neck. (b) The spiral neck with three turns. (c) A section of the curved tube.

Fig. 3 The equivalent Helmholtz resonator.

Fig. 4 Transmission loss of the HR with different extension neck lengths.

Fig. 5 Comparison of the analytical approach predictions and the FEM simulation for different extension neck lengths (solid lines represent the theoretical prediction, and dotted crosses represent the FEM simulation results).

Fig. 6 Comparison of the modified 1D analytical approach predictions and the experiment for a Helmholtz resonator with different extension lengths (the dotted symbols represent the experiment's results).

Fig. 7 Transmission loss of a Helmholtz resonator with a spiral neck.

Fig. 8 Comparison of predictions with FEM simulation for different spiral tube lengths (solid lines represent the theoretical prediction, and dotted crosses represent the FEM simulation results).

Fig. 9 Comparison of the HR with an extended neck and the HR with a spiral neck (dashed lines represent the HR with an extended neck, and solid lines represent the HR with a spiral neck).